JOURNAL OF THEORETICAL
AND APPLIED MECHANICS
52, 2, pp. 557-569, Warsaw 2014

NUMERICAL SIMULATION OF THE MICROPOLAR FLUID FLOW AND HEAT TRANSFER IN A CHANNEL WITH A SHRINKING AND A STATIONARY WALL

Kashif Ali, Muhammad Ashraf
Centre for Advanced Studies in Pure and Applied Mathematics, Bahauddin Zakariya University, Multan, Pakistan
e-mail: kashifali_381@yahoo.com

We present the numerical study of hydromagnetic (MHD) flow and heat transfer characteristics of a viscous incompressible electrically conducting micropolar fluid in a channel with one wall shrinking and the other at rest in the presence of a transverse applied magnetic field. Different from the classical shooting methodology, we employ a combination of a direct and an iterative method (SOR with optimal relaxation parameter) for solving the sparse systems of linear algebraic equations arising from the FD discretization of the linearized self similar nonlinear ODEs. Effects of some physical parameters on the flow and heat transfer are discussed and presented through tables and graphs. The present investigation may be beneficial to the flow and thermal control of polymeric processing.

Keywords: channel flow, shrinking/stationary walls, couple stress, quasi-linearization, Joule heating, viscous dissipation

1. Introduction

Flows through channels have attracted the research community due to their applications in the fields of binary gas diffusion, microfluidic devices, surface sublimation, ablation cooling, filtration, grain regression (as in the case of combustion in rocket motors) and the modeling of air circulation in the respiratory system (see Ashraf *et al.*, 2009b). Laminar air-flow systems have been used by the aerospace industry to control particulate contamination. Furthermore, the laminar flow cabinets have been used in the maintenance of negative pressure and in the adjustment of the fans to exhaust more air. Therefore, the Navier Stokes equations, which are the governing equations for these problems, have attracted the interest of the researchers. An exact solution of Navier Stokes equations for motion of an incompressible viscous fluid in a channel with different pressure gradients was presented by Suton and Barto (2008). Their solutions were helpful in verifying and validating computational models of complex unsteady flows to guide the design of fuel injectors and controlled experiments. Numerical simulation of flow through microchannels with design roughness was presented by Rawool *et al.* (2006). Recently, Hajipour and Dehkordi (2012) studied the transient behavior of fluid flow and heat transfer in vertical channels partially filled with a porous medium including the effects of inertial term and viscous dissipation.

All the studies cited above are limited to classical Newtonian fluids. There are many fluids which are important from the industrial point of view, and display non-Newtonian behavior. Due to the complexity of such fluids, several models have been proposed but the micropolar model is the most prominent one. Hoyt and Fabula (1964) experimentally predicted that the fluids which could not be characterized by Newtonian relationships indicated significant reduction in shear stress near a rigid body and could be well explained by the micropolar model introduced by Eringen (1964). MHD flow and heat transfer of a non-Newtonian fluid over a stretching/shrinking surface is important due to its engineering and industrial applications. For example, in the

extrusion of a polymer sheet from a dye, the sheet is sometimes stretched, whereas the properties of the end product depend considerably on the rate of cooling. The micropolar fluid is a hot area of research and therefore many investigators have studied the related flow and heat transfer problems. For example, Shangjun *et al.* (2006), Kelson *et al.* (2003), Naccache and Souza (2011), Ashraf *et al.* (2009a,b, 2011) and Ashraf and Batool (2013).

In the present paper, the hydromagnetic flow and heat transfer characteristics of a viscous electrically conducting incompressible micropolar fluid in a channel with a shrinking and a stationary wall are presented. Viscous dissipation and Joule heating effects have also been taken into account. A similarity transformation is used to convert the governing Navier-Stokes equations into a set of nonlinear ODEs, which are numerically solved using a computational procedure based on the quasi-linearization and finite difference discretization. The effects of the governing parameters on the flow and heat transfer aspects of the problem are discussed.

2. Mathematical formulation

We consider two dimensional hydromagnetic steady laminar viscous flow and heat transfer of an incompressible micropolar fluid in a parallel plate channel with the lower wall shrinking and the upper at rest, in the presence of a transverse applied magnetic field. The induced magnetic field is assumed to be negligible as compared with the imposed field. The magnetic Reynolds number which is the ratio of the product of characteristic length and fluid velocity to the magnetic diffusivity is assumed to be small. It is used to compare the transport of magnetic lines of the force in a conducting fluid, with the leakage of such lines from the fluid. For a small magnetic Reynolds number, the magnetic field will tend to relax towards a purely diffusive state. It is also assumed that there is no applied polarization and hence no electric field. The body couple is assumed to be absent. The two walls of the channel are located at $y=-a$ and $y=a$, where $2a$ is the channel width. We, therefore, may express the velocity $\underline{v}$ and the microrotation$\underline{\upsilon}$, respectively, in the following form

$$\underline{v}=(u(x,y),v(x,y),0) \qquad \underline{\upsilon}=(0,0,\phi(x,y)) \tag{2.1}$$

where ϕ is the component of the microrotation normal to the xy-plane.

Taking the viscous dissipation and Joule heating effects into consideration, the governing equations of the flow and heat transfer for the problem are

$$\begin{aligned}
&\frac{\partial u}{\partial x}+\frac{\partial v}{\partial y}=0\\
&u\frac{\partial u}{\partial x}+v\frac{\partial u}{\partial y}=\frac{-1}{\rho}\frac{\partial p}{\partial x}+\frac{\mu+\kappa}{\rho}\nabla^2 u+\frac{\kappa}{\rho}\frac{\partial \phi}{\partial y}-\frac{\sigma B_0^2}{\rho}u\\
&u\frac{\partial v}{\partial x}+v\frac{\partial v}{\partial y}=\frac{-1}{\rho}\frac{\partial p}{\partial y}+\frac{\mu+\kappa}{\rho}\nabla^2 v-\frac{\kappa}{\rho}\frac{\partial \phi}{\partial x}\\
&\rho j\Big(u\frac{\partial \phi}{\partial x}+v\frac{\partial \phi}{\partial y}\Big)=\gamma\nabla^2\phi+\kappa\Big(\frac{\partial v}{\partial x}-\frac{\partial u}{\partial y}\Big)-2\kappa\phi\\
&\rho c_p\Big(u\frac{\partial T}{\partial x}+v\frac{\partial T}{\partial y}\Big)=k_0\frac{\partial^2 T}{\partial y^2}+\mu\Big(\frac{\partial u}{\partial y}\Big)^2+\sigma B_0^2u^2
\end{aligned} \tag{2.2}$$

where ρ is the density, p is the pressure, μ is the dynamic viscosity, κ is the vortex viscosity, σ is the electrical conductivity, B_0 is the strength of the magnetic field, j is the micro-inertia density, γ is the spin gradient viscosity, c_p is the specific heat at constant pressure, κ_0 is the thermal conductivity and T is the temperature of the fluid. The boundary conditions for the velocity, microrotation and temperature fields for the present problem are

$$\begin{aligned} &u(x,-a) = -bx \qquad u(x,a) = 0 \qquad v(x,\pm a) = 0 \\ &\varphi(x,\pm a) = 0 \qquad T(x,-a) = T_1 \qquad T(x,a) = T_2 \end{aligned} \tag{2.3}$$

where $b > 0$ is the shrinking rate of the channel wall, and T_1 and T_2 (with $T_1 > T_2$) are fixed temperatures of the lower and upper channel walls, respectively. We define the following similarity variables to convert governing partial differential Eqs. (2.2) into ordinary differential equations

$$\begin{aligned} &\eta = \frac{y}{a} \qquad u = bxf'(\eta) \qquad v = -abf(\eta) \\ &\varphi = -\frac{b}{a}xg(\eta) \qquad \theta(\eta) = \frac{T - T_2}{T_1 - T_2} \end{aligned} \tag{2.4}$$

The above proposed velocity field is compatible with continuity Eq. (2.1) and, therefore, represents the possible fluid motion. After eliminating the pressure term from Eqs. $(2.2)_2$ and $(2.2)_3$, we introduce the above similarity transformation to the resulting equation to get

$$(1 + C_1)f^{iv} - C_1 g'' = \mathrm{Re}(f'f'' - ff''') + Mf'' \tag{2.5}$$

whereas Eqs. $(2.2)_4$ and $(2.2)_5$, in view of Eq. (2.4), are

$$C_3 g'' + C_1 C_2 (f'' - 2g) = f'g - fg' \qquad \theta'' + \mathrm{Pr}\,\mathrm{Re} f\theta' + \mathrm{Ec}\,\mathrm{Pr}(f''^2 + Mf'^2) = 0 \tag{2.6}$$

Here $C_1 = \kappa/\mu$ is the vortex viscosity parameter, $C_2 = \mu/(\rho j b)$ is the microinertia density parameter, $C_3 = \gamma/(\rho j a^2 b)$ is the spin gradient viscosity parameter, $\mathrm{Re} = \rho a^2 b/\mu$ is the Reynolds number, $\mathrm{Ec} = (bx)^2/[c_p(T_1 - T_2)]$ is the Eckert number, $\mathrm{Pr} = \mu c_p/\kappa_0$ is the Prandtl number and $M = a^2\sigma B_0^2/\mu$ is the magnetic parameter. Boundary conditions (2.3), in view of Eq. (2.4), in dimensionless form are reduced to

$$\begin{aligned} &f(\pm 1) = 0 \qquad f'(-1) = -1 \qquad f'(1) = 0 \\ &g(\pm 1) = 0 \qquad \theta(-1) = 1 \qquad \theta(1) = 0 \end{aligned} \tag{2.7}$$

3. Numerical solution

A usual approach is to write the nonlinear ODEs in form of a first order initial value problem as follows:

Setting: $f' = p$, $f'' = q$, $f''' = r$, $g' = s$, $\theta' = t$ in Eqs. (2.5) and (2.6), we have

$$\begin{aligned} &f' = p, \qquad p' = q \qquad q' = r \\ &r' = \frac{1}{1 + C_1}(\mathrm{Re}pq - \mathrm{Re}fr + Mq) + \frac{C_1}{(1 + C_1)C_3}(pg - fs - C_1C_2q + 2C_1C_2g) \\ &g' = s \qquad s' = \frac{1}{C_3}(pg - fs - C_1C_2q + 2C_1C_2g) \\ &\theta' = t \qquad t' = -\mathrm{Pr}\,\mathrm{Re}tf - \mathrm{Ec}\,\mathrm{Pr}(q^2 + Mp^2) \end{aligned} \tag{3.1}$$

with the following required boundary conditions

$$\begin{aligned} &f(-1) = 0 \qquad p(-1) = -1 \qquad g(-1) = 0 \qquad \theta(-1) = 1 \\ &q(-1) = \alpha_1 \qquad r(-1) = \alpha_2 \qquad s(-1) = \alpha_3 \qquad t(-1) = \alpha_4 \end{aligned} \tag{3.2}$$

Here, $\alpha_1, \alpha_2, \alpha_3, \alpha_4$ (that is $f''(-1)$, $f'''(-1)$, $g'(-1)$, $\theta'(-1)$) are the unknown initial conditions. Therefore, a shooting methodology is incorporated to solve the above system, which may be a

combination of the Runge Kutta method (to solve the 1st order ODEs) and a four dimensional zero finding algorithm (to find the missing conditions). It is worthy to note that the missing initial conditions are computed so that the solution satisfies the boundary conditions $f(1) = 0$, $p(1) = 0$, $g(1) = 0$, $\theta(1) = 0$, of the original boundary value problem.

A serious shortcoming of the shooting is the blowing up of the solution, before the initial value problem is completely integrated, and this happens quite often even with very accurate guesses for the initial conditions. This phenomenon is due to the instability of the differential equations and also because of the inherent strong dependence of the solution on the initial conditions of the problem. On the other hand, a finite difference method (FDM) does not suffer from this short-coming, and does have a chance as it tends to keep a firm hold on the entire solution at once.

Due to these features, it is desirable to incorporate the FDM in the computational procedure. Therefore, in our earlier works (Ashraf *et al.*, 2009a,b, 2011; Ashraf and Batool, 2013), we followed an approach different from the usual shooting method and involving the FDM, which we describe as follows:

An inspection of Eq. (2.5) reveals that it can be readily integrated, and becomes

$$(1 + C_1)f''' - C_1 g' - \mathrm{Re}(f'^2 - ff'') = \beta \tag{3.3}$$

where β is the constant of integration to be determined.

We consider this third order equation as the following system of coupled 1st and 2nd order ODEs

$$f' = p \qquad (1 + C_1)p'' - C_1 g' - \mathrm{Re}(p^2 - fp') = \beta \tag{3.4}$$

We solve these equations along with Eqs. (2.6), subject to the boundary conditions

$$\begin{aligned} &f(\pm 1) = 0 \qquad && p(-1) = -1 \qquad && p(1) = 0 \\ &g(\pm 1) = 0 \qquad && \theta(-1) = 1 \qquad && \theta(1) = 0 \end{aligned} \tag{3.5}$$

For the numerical solution of the present problem, we first discretize Eqs. (2.6) and $(3.4)_2$ at a typical grid point $\eta = \eta_i$ by employing central difference approximations for the derivatives. The resultant algebraic system is solved iteratively by the SOR method, subject to the appropriate boundary conditions given in Eq. (3.5). On the other hand, Eq. $(3.4)_1$ is integrated numerically by employing the 4th order Runge Kutta method, after every SOR iteration.

It is important to mention that the boundary condition $f_n = 0$ is used in finding the constant of integration β which is the only unknown as compared to the four missing initial conditions in the shooting approach. In our earlier work, we used the trial and error method to find β but some one dimensional zero finding algorithms may also be employed for the purpose. However, the sensitivity of β with respect to the governing parameters makes it difficult to find it, and some manual effort is always required in every simulation to obtain its desired value. That is why we need some alternative approach which does not require finding any unknown and is entirely based on the FDM. In this paper, we discuss an alternative approach based on the quasi-linearization of nonlinear ODEs.

3.1. Quasi-linearization method

In the quasi-linearization, we construct sequences of vectors $\{f^{(k)}\}$, $\{g^{(k)}\}$, $\{\theta^{(k)}\}$ which converge to the numerical solutions of Eqs. (2.5) and (2.6), respectively. To construct $\{f^{(k)}\}$, we linearize Eq. (2.5), by retaining only the first order terms, as follows:

We set

$$
\begin{aligned}
&G(f,f',f'',f''',f^{iv}) \equiv (1+C_1)f^{iv} + \mathrm{Re}ff''' - \mathrm{Re}f'f'' - Mf'' - C_1g'' \\
&G(f^{(k)}, f^{(k)'}f^{(k)''}, f^{(k)'''}, f^{(k)^{iv}}) + (f^{(k+1)} - f^{(k)})\frac{\partial G}{\partial f^{(k)}} + (f^{(k+1)'} - f^{(k)'})\frac{\partial G}{\partial f^{(k)'}} \\
&\quad + (f^{(k+1)''} - f^{(k)''})\frac{\partial G}{\partial f^{(k)''}} + (f^{(k+1)'''} - f^{(k)'''})\frac{\partial G}{\partial f^{(k)'''}} \\
&\quad + (f^{(k+1)^{iv}} - f^{(k)^{iv}})\frac{\partial G}{\partial f^{(k)^{iv}}} = 0 \\
&(1+C_1)f^{(k+1)^{iv}} + \mathrm{Re}f^{(k)}f^{(k+1)'''} - (\mathrm{Re}f^{(k)'} + M)f^{(k+1)''} - \mathrm{Re}f^{(k)''}f^{(k+1)'} \\
&\quad + \mathrm{Re}f^{(k)'''}f^{(k+1)} = \mathrm{Re}(-f^{(k)'}f^{(k)''} + f^{(k)}f^{(k)'''}) + C_1g^{(k)''}
\end{aligned}
\tag{3.6}
$$

Now Eqs. (3.6) gives a system of linear differential equations with f^k being the numerical solution vector of the k-th equation. To solve the ODEs, we replace the derivatives with their central difference approximations, giving rise to the sequence $\{f^{(k)}\}$, generated by the following linear system

$$
\mathbf{A}f^{(k+1)} = \mathbf{B} \qquad \text{with} \qquad \mathbf{A} = \mathbf{A}(f^{(k)}) \qquad \text{and} \qquad \mathbf{B} = \mathbf{B}(f^{(k)}, g^{(k)}) \tag{3.7}
$$

where n is the number of grid points. The matrices $\mathbf{A}_{n\times n}$ and $\mathbf{B}_{n\times 1}$ are initialized as follows

$$
\begin{aligned}
&A_{1,1} = 1 \qquad B_1 = 0 \\
&A_{2,1} = -4(1+C_1) + h\mathrm{Re}f_1 - Mh^2 \\
&A_{2,2} = 7(1+C_1) - h\mathrm{Re}f_2 + h^2\mathrm{Re}\alpha + \frac{h\mathrm{Re}}{2}f_4 + 2Mh^2 \\
&A_{2,3} = -4(1+C_1) - h\mathrm{Re}f_3 - Mh^2 \qquad A_{2,4} = 1 + C_1 + \frac{h\mathrm{Re}}{2}f_2 \\
&B_2 = h^2C_1(g_3 - 2g_2 + g_1) + \frac{h\mathrm{Re}}{2}f_2(-f_2 + 2f_1 - 2f_3 + f_4) \\
&\quad - \frac{h\mathrm{Re}}{2}(f_3 - f_1)(f_3 - 2f_2 + f_1) + 2h\alpha(1+C_1)
\end{aligned}
\tag{3.8}
$$

and for $2 < i < n-1$

$$
\begin{aligned}
&A_{i,i-2} = 1 + C_1 - \frac{h\mathrm{Re}}{2}f_i \qquad A_{i,i-1} = -4(1+C_1) + h\mathrm{Re}f_{i-1} - Mh^2 \\
&A_{i,i} = 6(1+C_1) + \frac{h\mathrm{Re}}{2}(f_{i+2} - f_{i-2}) + 2Mh^2 \\
&A_{i,i+1} = -4(1+C_1) - h\mathrm{Re}f_{i+1} - Mh^2 \qquad A_{i,i+2} = 1 + C_1 + \frac{h\mathrm{Re}}{2}f_i \\
&B_i = h^2C_1(g_{i+1} - 2g_i + g_{i-1}) + \frac{h\mathrm{Re}}{2}f_i(-f_{i-2} + 2f_{i-1} - 2f_{i+1} + f_{i+2}) \\
&\quad - \frac{h\mathrm{Re}}{2}(f_{i+1} - f_{i-1})(f_{i+1} - 2f_i + f_{i-1})
\end{aligned}
\tag{3.9}
$$

and

$$
\begin{aligned}
&A_{n-1,n-3} = 1 + C_1 - \frac{h\mathrm{Re}}{2}f_{n-1} \qquad A_{n-1,n-2} = -4(1+C_1) + h\mathrm{Re}f_{n-2} - Mh^2 \\
&A_{n-1,n-1} = 6(1+C_1) + \frac{h\mathrm{Re}}{2}(f_{i+2} - f_{i-2}) + 2Mh^2
\end{aligned}
$$

$$A_{n-1,n} = -4(1+C_1) - h\mathrm{Re} f_{i+1} - Mh^2 \tag{3.10}$$
$$B_{n-1} = h^2 C_1(g_{i+1} - 2g_i + g_{i-1}) + \frac{h\mathrm{Re}}{2} f_i(-f_{i-2} + 2f_{i-1} - 2f_{i+1} + f_{i+2})$$
$$-\frac{h\mathrm{Re}}{2}(f_{i+1} - f_{i-1})(f_{i+1} - 2f_i + f_{i-1})$$
$$A_{n,n} = 1 \qquad B_n = 0$$

(the superscripts have been dropped for simplicity and clarity).

On the other hand, Eqs. (2.6) are linear in g and θ, respectively. Therefore, in order to generate the sequences $\{g^{(k)}\}$ and $\{\theta^{(k)}\}$, these equations may be written as

$$\begin{aligned} &C_3 g^{(k+1)''} + C_1 C_2(f^{(k+1)''} - 2g^{(k+1)}) = f^{(k+1)'} g^{(k+1)} - f^{(k+1)} g^{(k+1)'} \\ &\theta^{(k+1)''} + \mathrm{Pr}\,\mathrm{Re} f^{(k+1)} \theta^{(k+1)'} + \mathrm{Ec}\,\mathrm{Pr}(f^{(k+1)''2} + M f^{(k+1)'2}) = 0 \end{aligned} \tag{3.11}$$

Importantly, $f^{(k+1)}$ is considered to be known in the above equations. We outline the computational procedure as follows:

- Provide the initial guess $f^{(0)}$, $g^{(0)}$ and $\theta^{(0)}$, satisfying the boundary conditions given in Eq. (2.7)
- Solve the linear system given by Eq. (3.7) to find $f^{(1)}$
- Use $f^{(1)}$ to solve the linear system arising from the FD discritization of Eqs. (3.11) to get $g^{(1)}$ and $\theta^{(1)}$
- Take $f^{(1)}$, $g^{(1)}$ and $\theta^{(1)}$ as the new initial guesses and repeat the procedure to generate the sequences $\{f^{(k)}\}$, $\{g^{(k)}\}$ and $\{\theta^{(k)}\}$ which, respectively, converge to f, g and θ (the numerical solutions of Eqs. (2.5) and (2.6))
- The three sequences are generated until

$$max\Big\{\|f^{(k+1)} - f^{(k)}\|_{L_\infty}, \|g^{(k+1)} - g^{(k)}\|_{L_\infty}, \|\theta^{(k+1)} - \theta^{(k)}\|_{L_\infty}\Big\} < 10^{-6}$$

It is important to note that the matrix $\mathbf{A}$ (in Eqs. (3.10)) is pentadiagonal and not diagonally dominant, and hence the SOR method may fail or work very poorly. Therefore, some direct method like LU factorization or Guassian elimination with full pivoting (to ensure stability) may be employed.

On the other hand, Eqs. (3.11) will give rise to the diagonally dominant algebraic system when discretized using the central differences. Therefore, we are in position to use the SOR method for these two equations. In this case, we also optimize the relaxation parameter ω by following Nakamura (1981). Instead of giving the details, we just outline the optimization procedure as follows:

— The SOR procedure is started with an initial guess for the value of the relaxation parameter ω to iteratively solve the linear system on some suitable basic grid.

— After each relaxation sweep except the first one, the quantities given by

$$\mu_\omega^{(t)} = \sqrt{\frac{N^{(t)}}{N^{(t-1)}}} \qquad \mu_J^{(t)} = \frac{\mu_\omega^{(t)} + \omega - 1}{\omega\sqrt{\mu_\omega^{(t)}}} \tag{3.12}$$

are computed, where

$$N^{(t)} = \sum_i (U_i^{(t)} - U_i^{(t-1)})^2 \tag{3.13}$$

Note that the upper index t stands for the relaxation sweep and the lower index i represents the grid point.

— The optimal relaxation parameter is then estimated from

$$\omega_{opt}^{(t)} = \frac{2}{1+\sqrt{1-(\mu_J^{(t)})^2}} \tag{3.14}$$

— The process of optimization is stopped once the criterion

$$|\mu_\omega^{(t)} - \mu_\omega^{(t-1)}| < \mathrm{TOL}_{\omega_{opt}} \tag{3.15}$$

is satisfied subject to $t > 1$ and $\mu_\omega^{(t)} < 1$. The iterative process is continued with $\omega = \omega_{opt}$ until convergence is achieved. $\mathrm{TOL}_{\omega_{opt}}$ is chosen to lie in the range $10^{-5} \leqslant \mathrm{TOL}_{\omega_{opt}} \leqslant 10^{-3}$ depending upon the density of the grid points. For a coarse grid, larger values result in rapid convergence while for a fine grid, smaller values may be chosen for better estimation of ω_{opt}.

We may improve the order of accuracy of the solution by solving the problem again on the grid with step $h/2$ and $h/4$, and then using the Richardson extrapolation which have been carried out at not only the common grid points but also at the skipped points, by following Roache and Knupp (1993). Any extrapolation scheme (Deuflhard, 1983) may be used for this purpose but we have used the polynomial extrapolation.

Moreover, a good initial guess for the solution on the finer grid can be obtained by injecting the previous coarse grid solution. Many operators may be found for this purpose but we have used the following linear operator which is simpler and easier to implement

$$W_{2i-1} \leftarrow U_i^c \qquad W_{2i} \leftarrow \frac{1}{2}(U_i^c + U_{i+1}^c) \tag{3.16}$$

where U^c represents the coarse grid solution and W is the required initial guess.

4. Results and discussion

The physical quantities of our interest are the shear stresses, the couple stresses and the heat transfer rates at the channel walls which are, respectively, proportional to the values of f'', g', θ' at the two walls. The parameters of the problem are the Reynolds number Re, the magnetic parameter M, the Prandtl number Pr, the Eckert number Ec and the micropolar parameters C_1, C_2 and C_3. These parameters are all dimensionless groups of material and flow properties, and/or geometric dimensions of the domain. The traditional way (e.g., Lok *et al.*, 2007) of studying flow and thermal characteristics of the fluid dynamics problems is to specify the values of these dimensionless groups rather than specifying the particular fluid properties and the domain dimensions. Obviously, the results obtained in this way are applicable to the flow problems with particular values of material properties and the dimensions of the domain, falling in the ranges considered in the studies. In the present work we have computed our results for the following values of the governing parameters: $M = 0, 10, 20, 30, 40, 50$, $\mathrm{Re} = 1, 5, 10, 20, 30, 40, 50$, $\mathrm{Ec} = 0, 1, 2, 3, 4$ and $\mathrm{Pr} = 0.1, 0.5, 1, 2, 2.5$.

We shall study the effects of the parameters on $f''(\pm 1)$, $g'(\pm 1)$ and $\theta'(\pm 1)$ as well as on the velocity profiles $f(\eta)$, $f'(\eta)$, the microrotation profile $g(\eta)$ and the heat profile $\theta(\eta)$.

All the cases of the micropolar parameters in the present work are shown in Table 1, whereas the first case corresponds to the Newtonian fluid. Table 2 shows the convergence of our numerical results as the step-size decreases, which gives us confidence on our computational procedure.

The magnetic field exerts a force, called the Lorentz force, which tends to drag the fluid towards the shrinking wall, which not only results in increasing the shear stress at the wall but also causes greater spinning of the micro fluid particles, and hence increases the couple stress as well (clear from Table 3). Moreover, the frictional force raises the temperature of the

Table 1. Five cases of values of micropolar parameters C_1, C_2 and C_3

Cases	C_1	C_2	C_3
1(Newtonian)	0	0	0
2	2	0.7	0.3
3	4	1.5	0.7
4	6	2.0	1.5
5	8	2.5	2.0

Table 2. Dimensionless temperatures $\theta(\eta)$ on three grid sizes and extrapolated values for $C_1 = 4$, $C_2 = 1.5$, $C_3 = 0.7$, $\mathrm{Re} = 50$, $M = 1$, $\mathrm{Ec} = 0.5$ and $\mathrm{Pr} = 0.5$

$\theta(\eta)$				
η	1st grid η ($h = 0.02$)	2nd grid ($h = 0.01$)	3rd grid ($h = 0.005$)	Extrapolated values
-0.8	1.015900	1.015916	1.015920	1.015921
-0.6	1.028347	1.028372	1.028379	1.028381
-0.4	1.039211	1.039244	1.039252	1.039255
-0.2	1.048684	1.048721	1.048731	1.048734
0	1.056010	1.056130	1.056137	1.056140
0.2	1.056186	1.056160	1.056153	1.056151
0.4	1.018667	1.018485	1.018439	1.018424
0.6	0.856763	0.856441	0.856361	0.856334
0.8	0.497270	0.497052	0.496996	0.496978

Table 3. The effect of the magnetic field on shear and couple stresses and the heat transfer rate with $C_1 = 3$, $C_2 = 0.8$, $C_3 = 1$, $\mathrm{Re} = 20$, $\mathrm{Ec} = 0.5$ and $\mathrm{Pr} = 0.1$

M	$f''(-1)$	$f''(1)$	$g'(-1)$	$g'(1)$	$\theta'(-1)$	$\theta'(1)$
0	0.297547	-2.871344	1.750801	3.082036	0.080047	-6.683872
10	0.663511	-2.214353	2.239587	2.458181	2.738352	-7.638689
20	1.082883	-1.736506	2.711143	1.970446	5.237685	-8.024192
30	1.509880	-1.412842	3.125411	1.616686	7.576004	-8.148545
40	1.915830	-1.197936	3.472198	1.366667	9.766241	-8.181408

fluid which results in increasing the temperature difference between the channel walls and the fluid. Therefore, the heat transfer rate at the two walls, which is directly proportional to the temperature difference, also increases.

Table 4 predicts that the shear and couple stresses as well as the heat transfer rate at the shrinking wall may decrease as the Reynolds number increases. The increased shrinking rate of the wall forces the fluid to move rapidly away from the shrinking wall, thus decreasing both the shear and couple stresses. Also, the fluid carries away heat (generated due to the Joule heating effect) from the region near the lower wall, thus decreasing the temperature difference and hence the heat transfer rate at the shrinking wall. On the other hand, the incoming of the heated fluid towards the upper wall increases not only the shear and couple stresses but also the heat transfer rate.

It is clear from Table 5 that the micropolar structure of the fluid tends to reduce the shear stress at the shrinking wall without significantly altering the shear stress at the stationary wall. This is in accordance with the experimental prediction of Hoyt and Fabula (1964) that the micro fluid particles cause significant reduction in the shear stress near a moving rigid surface. Moreover, the particles also cause microrotation in the fluid which is responsible for the couple

Table 4. The effect of the Reynolds number on shear and couple stresses and the heat transfer rate with $C_1 = 3$, $C_2 = 0.8$, $C_3 = 1$, $M = 5$, $\mathrm{Ec} = 0.5$ and $\mathrm{Pr} = 0.1$

Re	$f''(-1)$	$f''(1)$	$g'(-1)$	$g'(1)$	$\theta'(-1)$	$\theta'(1)$
1	2.048361	−0.780919	3.566882	1.130933	7.995645	−3.260171
10	1.755744	−0.941748	3.330322	1.306377	5.654433	−4.520490
20	1.431412	−1.174269	3.045316	1.545727	4.325219	−5.211422
30	1.127477	−1.471094	2.752210	1.830289	3.562179	−5.952669
40	0.867088	−1.825513	2.476137	2.143552	3.072278	−6.776226

Table 5. The effect of micropolar coefficients on shear and couple stresses and the heat transfer rate with $\mathrm{Re} = 5$, $M = 20$, $\mathrm{Pr} = 0.5$ and $\mathrm{Ec} = 0.5$

Case	$f''(-1)$	$f''(1)$	$g'(-1)$	$g'(1)$	$\theta'(-1)$	$\theta'(1)$
1	4.516739	−0.711734	0	0	0.759419	−0.738241
2	2.895274	−0.764749	2.720250	0.561054	0.839335	−0.900799
3	2.365865	−0.773087	3.499924	1.040502	0.910777	−0.979324
4	2.149622	−0.774630	3.576582	1.049530	0.953960	−1.029429
5	1.981817	−0.781593	3.871003	1.273793	0.986792	−1.061255

Table 6. The effect of the Eckert number on the heat transfer rate with $C_1 = 3$, $C_2 = 0.8$, $C_3 = 1$, $\mathrm{Re} = 10$, $M = 1$ and $\mathrm{Pr} = 0.1$

Ec	$\theta'(-1)$	$\theta'(1)$
0	−0.393561	−0.581297
1	−0.235738	−0.662955
2	−0.077915	−0.744612
3	0.079908	−0.826269
4	0.237731	−0.907926

Table 7. The effect of the Prandtl number on heat transfer rate with $C_1 = 3$, $C_2 = 0.8$, $C_3 = 1$, $\mathrm{Re} = 10$, $M = 1$ and $\mathrm{Ec} = 3$

Pr	$\theta'(-1)$	$\theta'(1)$
0.1	0.079908	−0.826269
0.5	1.909219	−2.200202
1	3.321423	−3.787488
2	4.990100	−6.302292
2.5	5.615060	−7.350247

stress at the walls. The micropolar structure also tends to increase the heat transfer rate at the two walls by raising the temperature distribution across the channel. On the other hand, it is evident from Table 6 that the viscous dissipation may cause thermal reversal near the shrinking wall only, which is supported by the Prandtl number as predicted in the Table 7.

The streamlines for the present problem are shown in Fig. 1. On the other hand, Figs. 2 and 3 show that the external magnetic field reduces the two velocities (normal and streamwise) while raising the fluid temperature, whereas it raises the microrotation profiles only in a smaller region near the shrinking wall. Moreover, it supports the thermal reversal near the shrinking wall, due to the viscous dissipation and Joule heating effects.

Figures 4 and 5 show that the influence of the Reynolds number on the problem is almost opposite to that of the magnetic field, with temperature distribution near the upper wall being

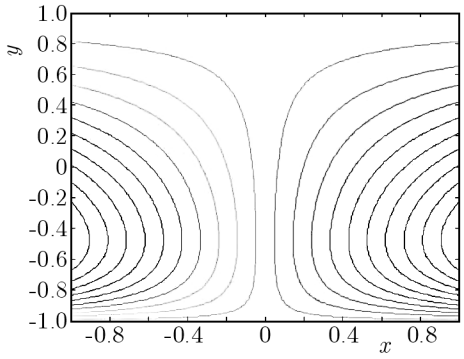

Fig. 1. Streamlines for the problem for $C_1 = 4$, $C_2 = 1.5$, $C_3 = 0.7$, R = 1 and $M = 50$

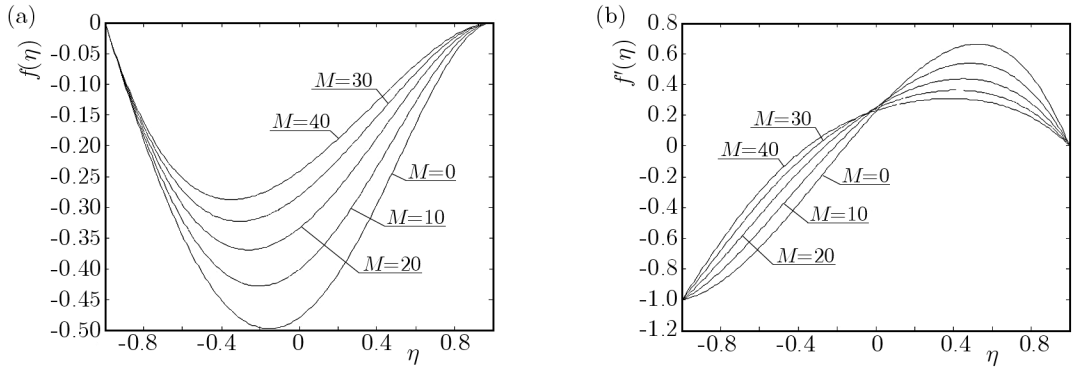

Fig. 2. Streamwise (a) and normal (b) velocity profiles for $C_1 = 4$, $C_2 = 1.5$, $C_3 = 0.7$, Re = 50, Ec = 1, Pr = 2.5 and various M

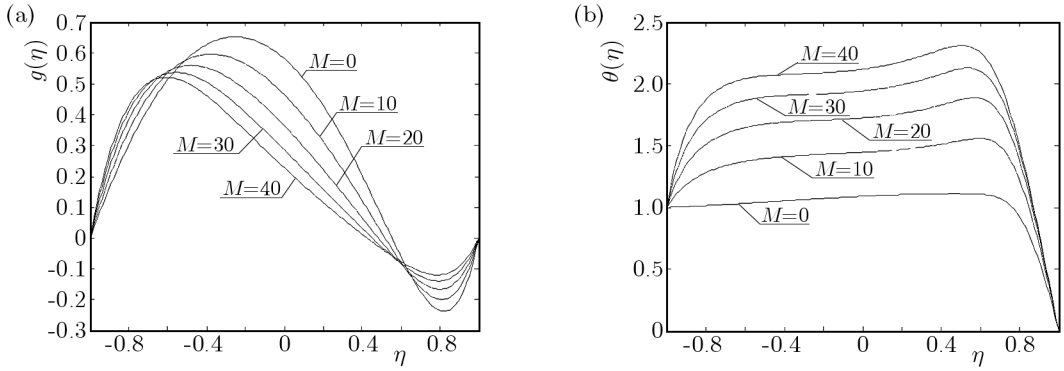

Fig. 3. Microrotation (a) and temperature (b) profiles for $C_1 = 4$, $C_2 = 1.5$, $C_3 = 0.7$, Re = 50, Ec = 1,Pr = 2.5 and various M

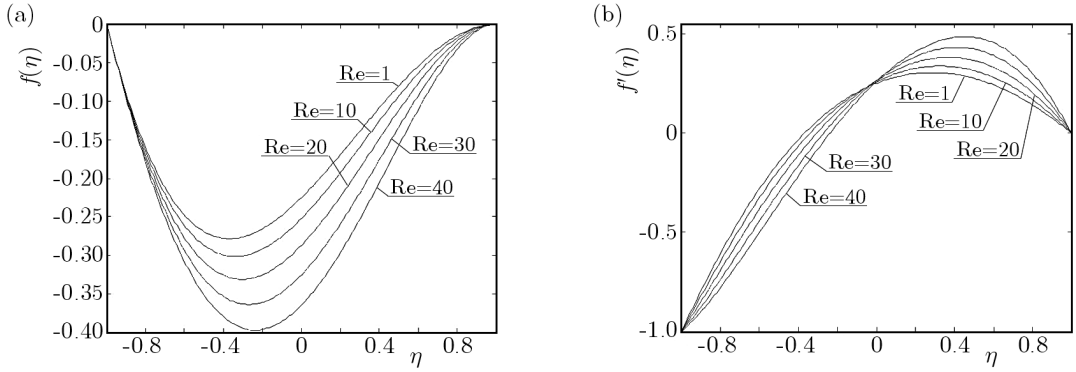

Fig. 4. Normal (a) and streamwise (b) velocity profiles for $C_1 = 4$, $C_2 = 1.5$, $C_3 = 0.7$, $M = 10$, Ec = 1, Pr = 2.5 and various Re

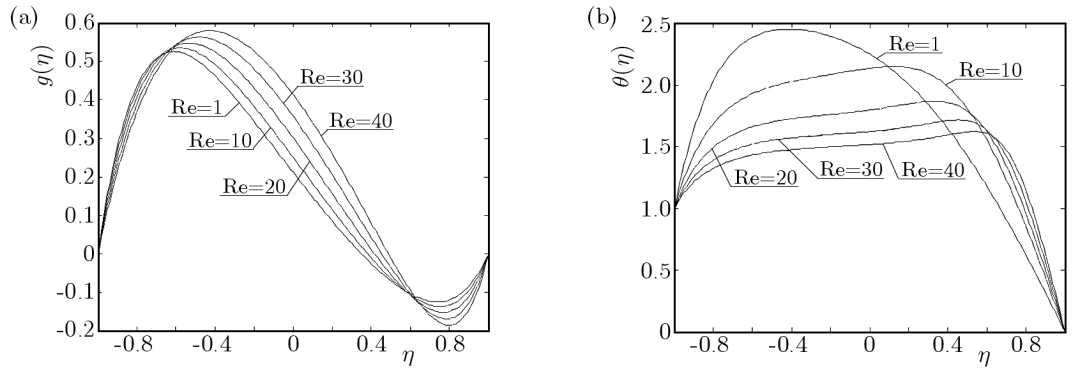

Fig. 5. Microrotation (a) and temperatue (b) profiles for $C_1 = 4$, $C_2 = 1.5$, $C_3 = 0.7$, $M = 10$, $\mathrm{Ec} = 1$, $\mathrm{Pr} = 2.5$ and various Re

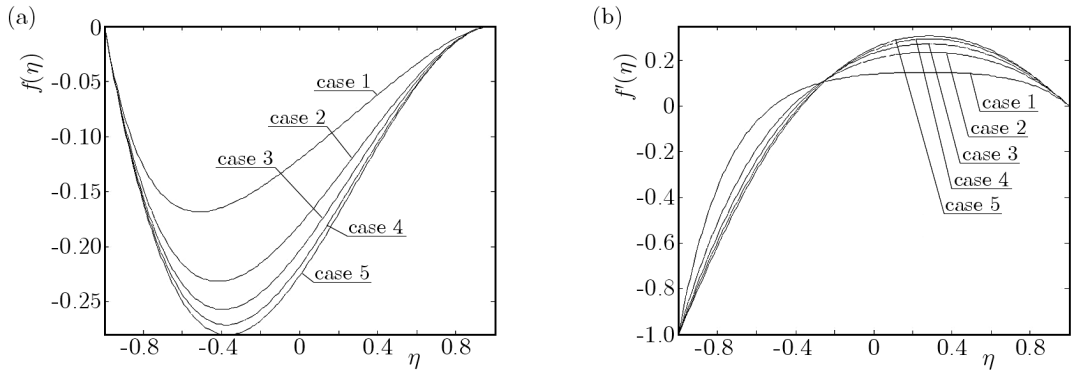

Fig. 6. Normal (a) and streamwise (b) velocity profiles for $M = 20$, $\mathrm{Ec} = 1$, $\mathrm{Re} = 5$, $\mathrm{Pr} = 2.5$ and various cases of the micropolar parameters

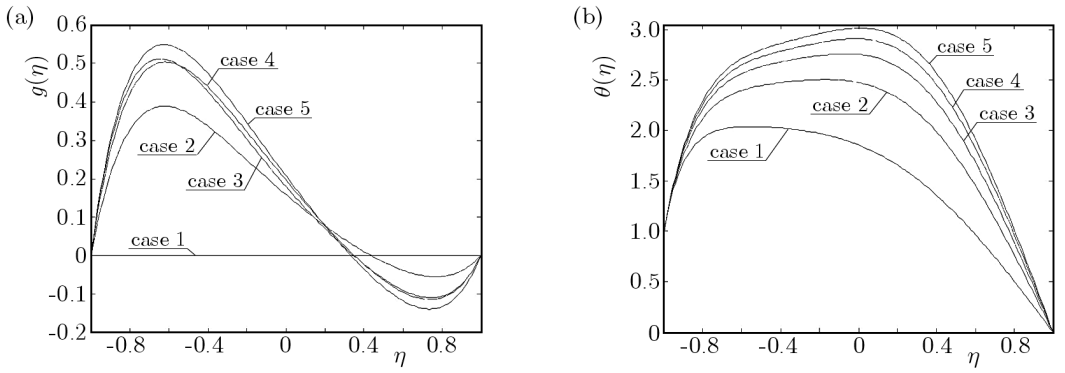

Fig. 7. Microrotation (a) and temperatue (b) profiles for $M = 20$, $\mathrm{Ec} = 1$, $\mathrm{Re} = 5$, $\mathrm{Pr} = 2.5$ and various cases of the micropolar parameters

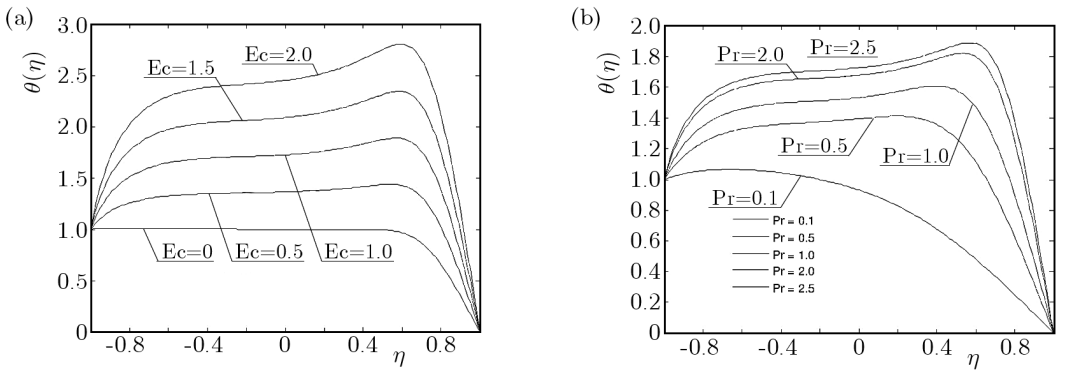

Fig. 8. Temperature profiles for: (a) $C_1 = 4$, $C_2 = 1.5$, $C_3 = 0.7$, $\mathrm{Re} = 50$, $\mathrm{Pr} = 2.5$, $M = 20$ and various Ec, (b) $C_1 = 4$, $C_2 = 1.5$, $C_3 = 0.7$, $\mathrm{Re} = 50$, $\mathrm{Ec} = 1$, $M = 20$ and various Pr

the only exception. It is clear from Figs. 6 and 7 that the micropolar structure of the fluid increases the velocity, microrotation and temperature distributions across the channel. Finally, Fig. 8a shows that the viscous dissipation may cause thermal reversal near the shrinking wall by significantly raising the temperature profiles, which is supported by the Prandtl number as predicted by the Fig. 8b.

5. Conclusions

We have numerically studied the problem of a viscous incompressible electrically conducting micropolar fluid in a channel with one wall shrinking and the other at rest. It has been observed that the external magnetic field tends to raise the microrotation profiles only in a smaller region near the shrinking wall. Moreover, it tends to balance the influence of the shrinking channel wall on the flow and heat transfer characteristics of the problem. The combined effect of viscous dissipation and Joule heating may raise the temperature distribution to such an extent that thermal reversal may occur near the shrinking wall, which is supported by both the Prandtl number and the micropolar structure of the fluid.

Acknowledgements

The authors are extremely grateful to the Higher Education Commission of Pakistan for the financial support to carry out this research. The authors are also very grateful to the learned reviewer for the useful comments improving the quality of the paper.

References

1. Ashraf M., Batool K., 2013, MHD flow and heat transfer of a micropolar fluid over a stretchable disk, *Journal of Theoretical and Applied Mechanics*, **51**, 25-38
2. Ashraf M., Kamal M.A., Syed K.S., 2009a, Numerical simulation of a micropolar fluid between a porous disk and a non-porous disk, *Journal of Applied Mathematics and Modelling*, **33**, 1933-1943
3. Ashraf M., Kamal M.A., Syed K.S., 2009b, Numerical study of asymmetric laminar flow of micropolar fluids in a porous channel, *Computers and Fluids*, **38**, 1895-1902
4. Ashraf M., Kamal M.A., Syed K.S., 2011, Numerical simulation of flow of micropolar fluids in a channel with a porous wall, *International Journal for Numerical Methods in Fluids*, **66**, 906-918
5. Deuflhard P., 1983, Order and step-size control in extrapolation methods, *Numerical Mathematics*, **41**, 399-422
6. Eringen A.C., 1964, Simple micropolar fluids, *International Journal of Engineering Science*, **2**, 205-217
7. Hajipour M., Dehkordi A.M., 2012, Transient behavior of fluid flow and heat transfer in vertical channel partially filled with porous medium: Effects of inertial term and viscous dissipation, *Energy Conversion and Management*, **61**, 1-7
8. Hoyt J.W., Fabula A.G., 1964, The effect of additives on fluid friction, *US Naval Ordinance Test Station Report*
9. Kelson N.A., Desseaux A., Farrell T.W., 2003, Micropolar flow in a porous channel with high mass transfer, *ANZIAM*, **44**, 479-495
10. Lok Y.Y., Ioan P., Chamkha A.J., 2007, Non-orthogonal stagnation point flow of a micropolar fluid, *International Journal of Engineering Science*, **45**, 173-184
11. Naccache M.F., Souza P.R., 2011, Heat transfer to non-Newtonian fluids in laminar flow through rectangular ducts, *International Journal of Thermal Sciences*, **8**, 16-25

12. Nakamura S., 1991, *Applied Numerical Methods with Software*, Prentice-Hall, 442-446

13. Rawool A.S., Mitra S.K., Kandlikar S.G., 2006, Numerical simulation of flow through microchannels with designed roughness, *Microfluidics and Nanofluidics*, **2**, 215-221

14. Roache P.J., Knupp P.M., 1993, Completed Richardson extrapolation, *Communications in Numerical Methods in Engineering*, **9**, 365-374

15. Shangjun Y., Kequn Z., Wang W., 2006, Laminar flow of micropolar fluid in rectangular microchannels, *Acta Mechanica Sinica*, **22**, 403-408

16. Sutton R.S., Barto A.G., 2008, Exact Navier-Stokes solution for pulsatory viscous channel flow with arbitrary pressure gradient, *Journal of Propulsion and Power*, **24**, 1412-1423

Manuscript received June 3, 2013; accepted for print December 6, 2013